

## Electronic Supplementary Information

The effect of solid electrolyte interphase on the mechanism of operation of lithium-sulfur batteries.

E. Markevich<sup>\*a</sup>, G. Salitra<sup>\*a</sup>, A. Rosenman<sup>a</sup>, Y. Talyosef<sup>a</sup>, F. Chesneau<sup>b</sup> and D. Aurbach<sup>\*a</sup>

<sup>a</sup>Department of Chemistry Bar-Ilan University, Ramat Gan 52900 Israel

markeve@biu.ac.il, salitrg@biu.ac.il, Doron.Aurbach@biu.ac.i

<sup>b</sup>BASF SE, Ludwigshafen 67056, Germany

Fig. S1 and S2 show SEM images of AC1 and EDX mapping of sulfur distribution in the sulfur-carbon composite powders and sulfur-carbon composite electrodes.

Fig. S3 shows the XRD patterns of the sulfur powder used, exhibiting its crystalline structure, pristine AC1 and sulfur-AC1 composite, as indicated. XRD patterns of pristine AC1 powder (Fig. S3) reveals no (002) diffraction peak. X-ray diffraction patterns of AC1 pristine powder, elemental sulfur powder and composite AC1-sulfur powders with different wt. % of sulfur are shown in Fig. S3. XRD patterns of the sulfur powder exhibit its crystalline structure. XRD patterns of pristine AC1 powder reflect the totally disordered structure of AC1 carbon. Empirical parameter R defined as the ratio of the height of (002) Bragg peak to the background is close to approximately ~1 for this powder <sup>[1]</sup> due to almost randomly oriented graphene sheets arranged as single layers. No

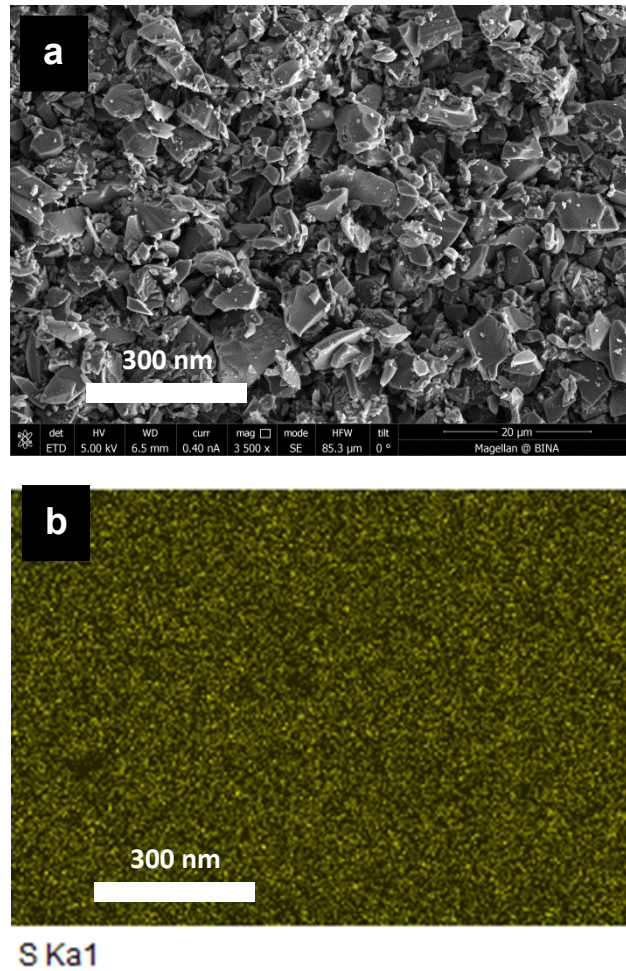
crystalline sulfur peaks were detected in the sulfur-AC1 composite powders. Broad peak at about 25° corresponds to a highly.

Fig. S4 shows the TGA curves of sulfur-AC1 powders with 40, 50 and 60 wt% sulfur, with weight loss exactly corresponding to sulfur content in these composite powders.

We compared several types of separators in terms of their wettability and resistance. Polyethylene separator (PE) (Tonen) is not wettable by IL electrolyte at all. Polypropylene (PP) (Celgard), thickness 25  $\mu\text{m}$ , and polyolefin  $\text{SiO}_2$  containing separator Entek, thickness 25  $\mu\text{m}$ , are wettable with IL electrolyte solution. The results of the measurements of high frequency resistance as a function of number of separator layers are shown in Fig. S6. The resistance of 1 layer of PP separator comprised 2.1 Ohm, and for 1 layer of Entek separator 0.34 Ohm.

### References Cited

1. Y. Liu, J. S. Xue, T. Zheng, J. R. Dahn, *Carbon* **1996**, 34, 193.

**Sulfur-AC1 composite powder**

**Fig. S1.** SEM images of sulfur-AC1 (a) composite powders and EDX mapping of the sulfur distribution in the sulfur-carbon composites prepared with AC1 (b).

### Sulfur-AC1 composite electrode

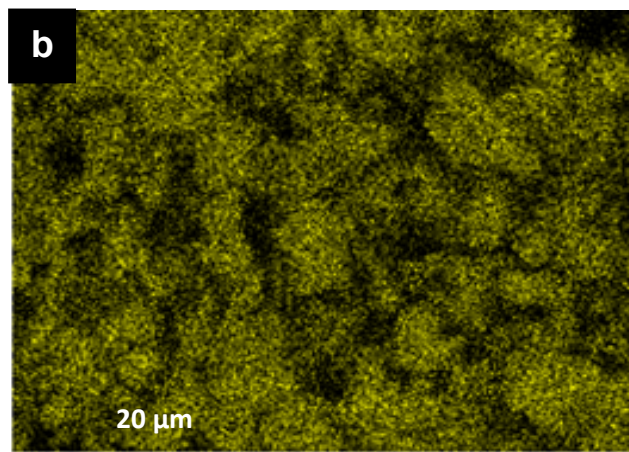
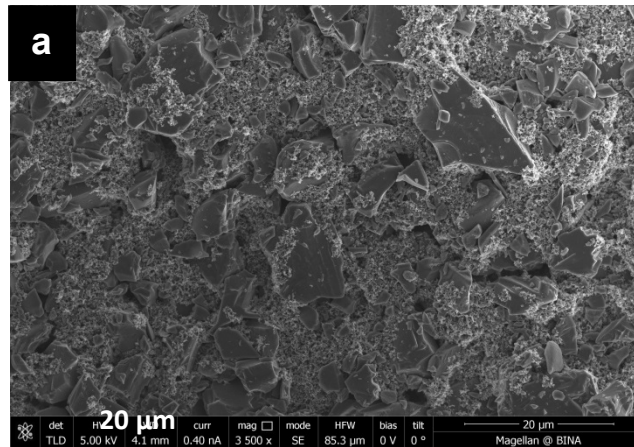


**Fig. S2.** SEM images of sulfur-AC1 composite electrodes (a) and EDX mapping of the sulfur distribution in the sulfur-carbon composite electrodes prepared with sulfur-AC1 (b).

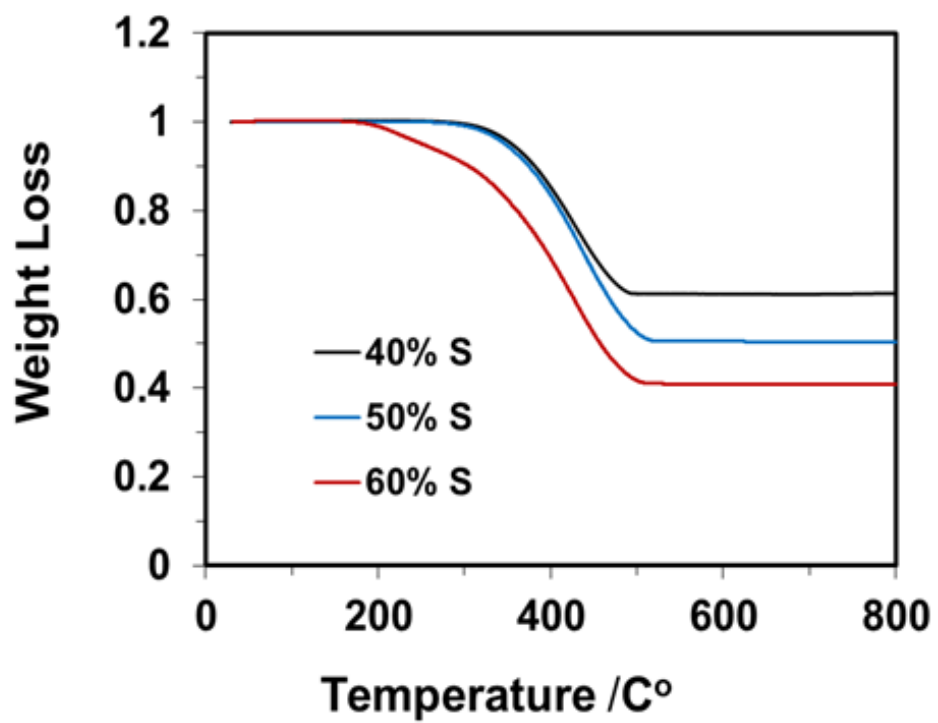


**Fig. S3.** TGA curves of sulfur-AC1 composite powders with different wt% of sulfur, as indicated.

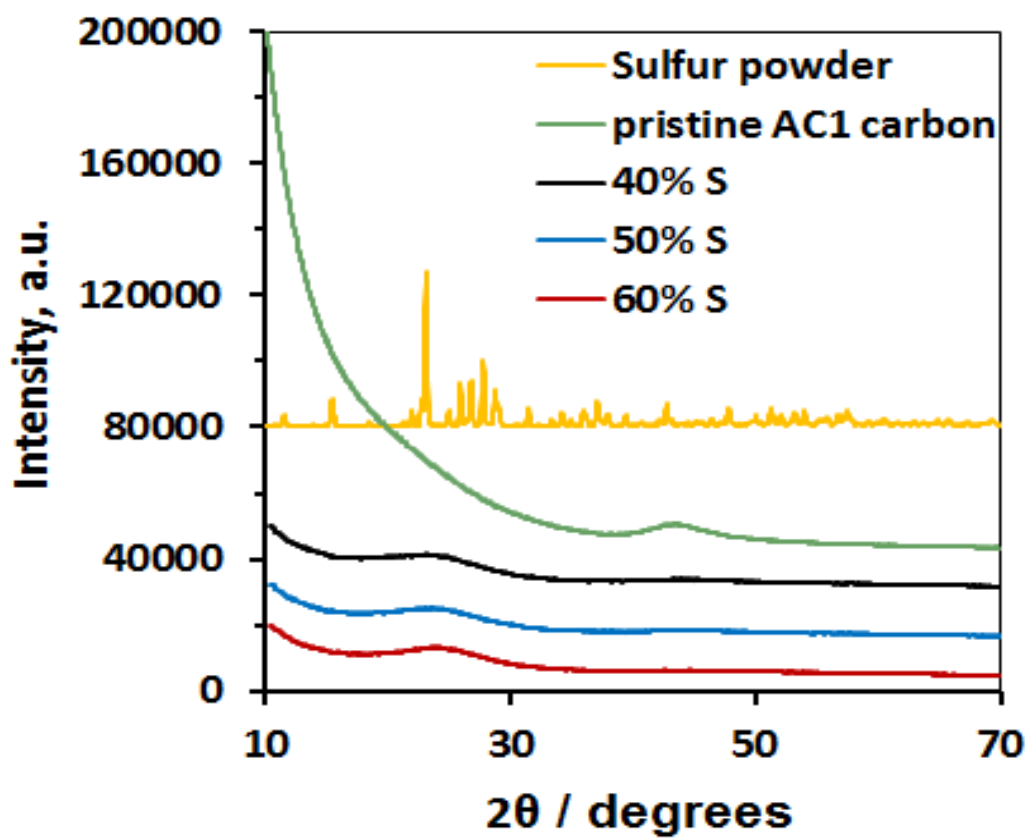


**Fig. S4.** X-ray diffraction patterns of AC1 powder, elemental sulfur powder and composite AC1-sulfur powders with different wt% of sulfur, as indicated.

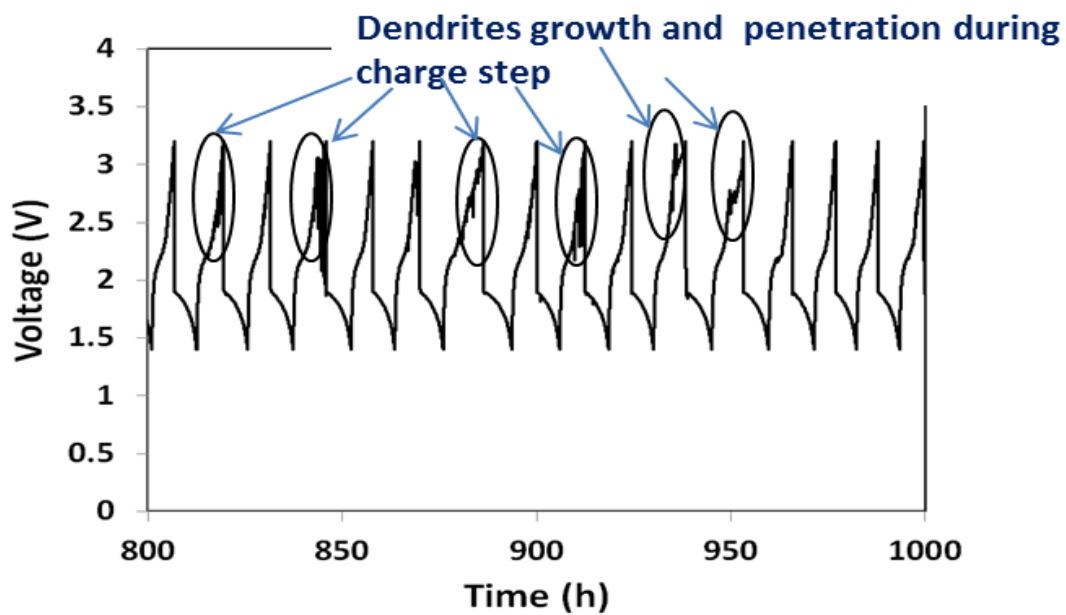


**Fig. S5.** Typical voltage profile obtained during galvanostatic cycling for Li-S/AC1 cells at 30°C in 0.5M Li FSI in MPP FSI electrolyte solution with the use of quartz separators. Current density: 50 mA $g^{-1}$  sulfur.

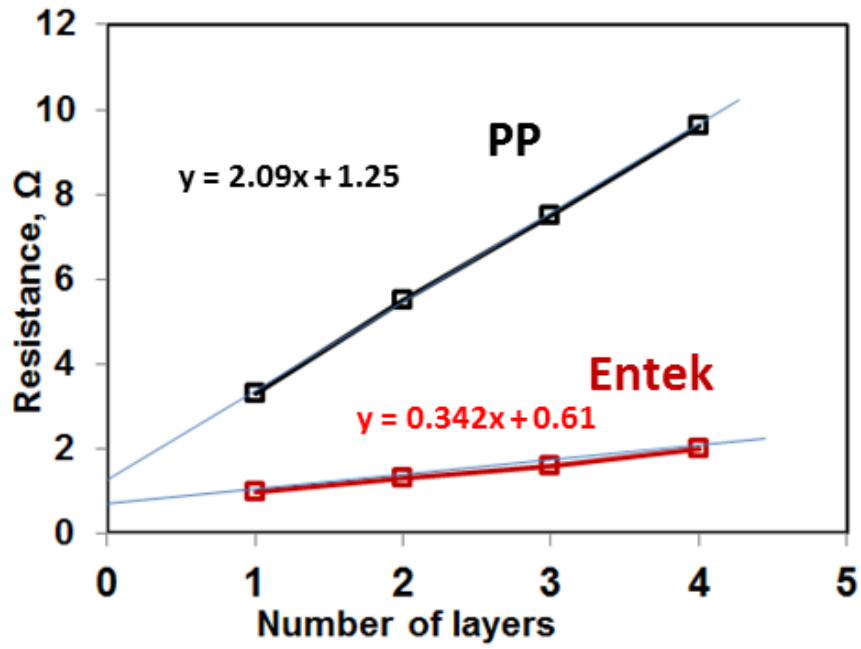


**Fig. S6.** High frequency resistance as a function of number of separator layers measured for polypropylene (PP) and Entek separators, as indicated



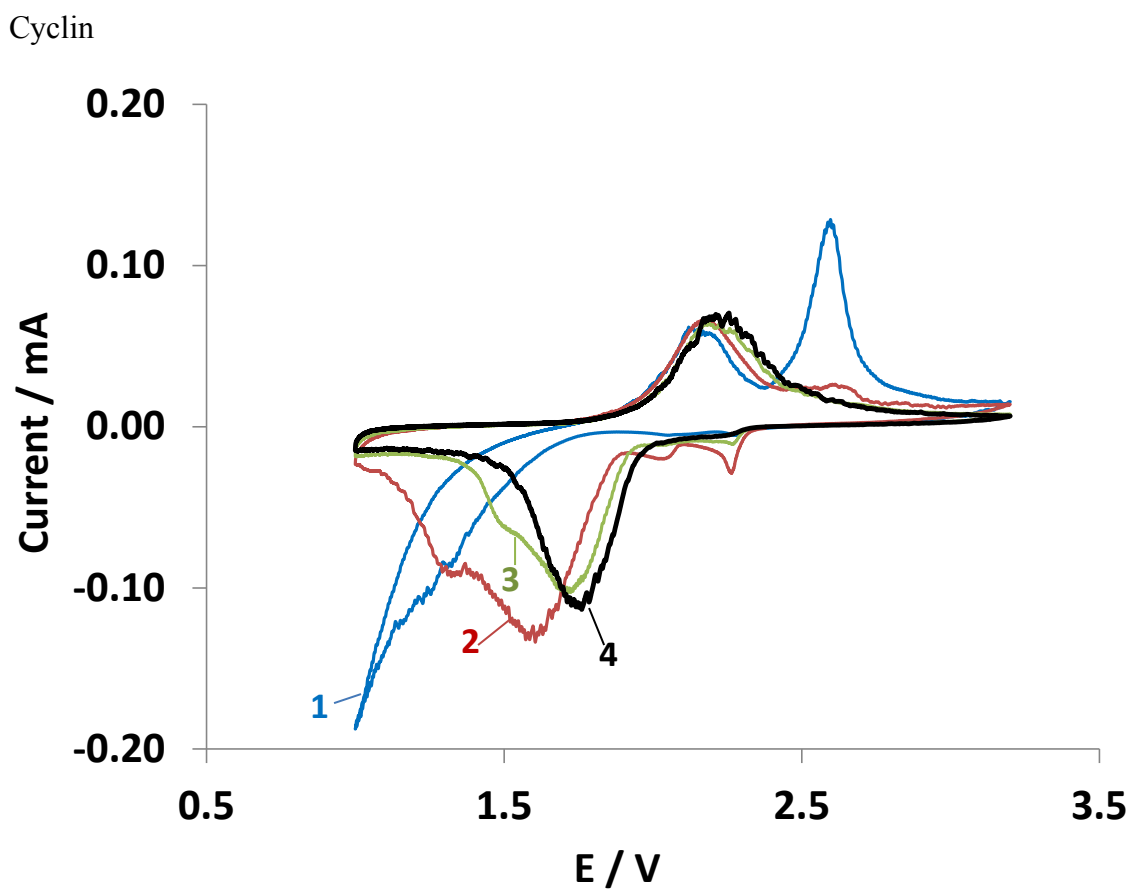


**Fig.S7.** Cyclic voltammogrammes of composite S-C electrode recorded during four initial cycles (as indicated) at a scan rate of  $15 \mu\text{Vs}^{-1}$  in 0.5M Li FSI in MPP FSI electrolyte solution,  $25^\circ\text{C}$ .